Soft, Stretchable and Wireless Sensor Patch with Digitally Printed Liquid Metal Alloy Interconnects

Jan Maslik, Oskar Hellman*, Bei Wang*, Alessandro Gumiero†, Luigi Dellatorre†, Gustaf Mårtensson‡ and Klas Hjort**
*Division of Microsystems Technology, Department of Materials Science and Engineering
Ångström Laboratory, Uppsala University, 751 03 Uppsala, Sweden
Email: jan.maslik@angstrom.uu.se
†STMicroelectronics, 208 64 Agrate Brianza, MB, Italy
‡Mycronic AB, 183 03 Täby, Sweden

Abstract— Characteristics of high electrical conductivity, high strain tolerance and resistance to fatigue are vital for electronic circuits of on-skin wearable systems. Gallium-based liquid metals offer a unique combination of these characteristics making them excellent alternatives to conventional conductive stretchable inks. In order to obtain better wearing experience, it is advantageous to fabricate devices using breathable materials. However, effective automation solutions for the production of high-resolution digitally patterned circuits for soft and stretchable devices remain a challenge. The presented manufacturing strategy involves adopting a needle dispensing technique for the precise patterning of liquid metal conductors. The circuitry is deposited onto a soft, thin and highly breathable polyurethane medical film. Further, we investigate and map conditions of reliable printing of liquid metal on the polyurethane film for two sizes of dispensing needles with inner diameters of 150 µm and 360 µm. Despite the increased porosity and surface roughness associated with the high breathability of the film, it is possible to reliably deposit liquid metal interconnects with a line width and height below 100 µm. The technological solution results in a first demonstrator presented: an electrophysiological patch.

Keywords—wearable electronics, soft electronics, digital printing, liquid metal patterning

I. Introduction

Monitoring of biometrics is a rapidly growing field in both sports, healthcare, as well as in everyday life. Providing high compliance and comfort, soft and stretchable wireless sensors and smart patches open up for new applications in the realm of wearable electronics [1 - 4].

The presented wearable device, consisting of a disposable patch and reusable electronic modules, acquires signals of the electrical activity of the heart, wirelessly streams data to a computer, and displays a real-time electrocardiogram. To link the two parts of the device, the patch carries a small and thin flexible circuit with a mounted rigid connector. The assembly of the device takes place on a large area stretchable carrier, approximately an A4 size, and is performed by automated pick-n-place technology. Digitally printed liquid metal (LM) traces serve as compliant electrical interconnects between the epidermal ECG electrodes and the flexible circuit with the rigid connector.

The reusable modules are of two kinds. The first module contains a sensor and data collecting circuit board with Bluetooth communication capabilities. The second module consists of a rechargeable cell battery that functions as a power supply for the sensor module. Both the sensor board and the battery are mounted on a thin flexible board with a rigid connector through which the modules can be coupled together and with the patch. The whole rigid-flex assembly is embedded in a soft silicone gel with a low-friction polyurethane coating contributing to the unobtrusiveness of the device for a wearer.

The most common method to fabricate stretchable electronics is to use meandering spring structures of thin solid conductors. Circuits of this kind are often limited to low elongations with out-of-plane deformation due to the yield strain of the conductor. As a consequence, contact fatigue of integrated rigid components yield from cyclic strain [5 - 6]. In addition, these thin meandering interconnects need a larger footprint and have higher electrical resistance than those in normal rigid and flexible circuits.

Allowing for straight lines and large cross sections with high compliance, LM conductors of gallium-based alloys, such as E-GaIn or Galinstan, show excellent electrical and thermal characteristics, which makes them good candidates for use in soft and compliant electronics for biometric sensing. However, circuits of LM are challenging to manufacture with conventional PCB technologies and therefore the focus of this study is on the digital printing of the LM for the disposable patch. Various deposition technologies and methods have in the recent years been studied and the patterning techniques can be divided into two main groups, i.e., masked deposition [7 - 8] and digital printing. Digital printing has been demonstrated by ink jet printing and needle dispensing [9 - 12].

As previously studied, the deposition of liquid metals through needle dispensing is driven by a shearing mechanism rather than a volumetric or pressure displacement mechanism typical for viscoelastic liquids. Parameters like print height and applied extruding pressure are crucial for quality and reliable patterning. Galinstan naturally forms a nanometer thin oxide layer when in contact with air, and the hydrophilic nature of this oxide contacting the surface allows for adhesion of the liquid metal to many substrates during deposition [13]. The choice of substrate material and its surface conditions are therefore also of importance for reliable and consistent deposition. The parameters of acceleration and deposition speed have no significant effect on the geometry of the patterned structures and therefore no attention is paid to it [14 - 15].

II. Experimental

A. Substrate preparation

Substrates for patterning were prepared by spin coating of approximately 100 µm films of PDMS Sylgard 182 (DOW, Michigan, USA) on 10 × 10 cm glass panes. Thermoplastic polyurethane film, Inspire®2150 (TC Transcontinental, Montréal, Canada) cut to size and removed from its paper liner was transferred to the PDMS coated glass to electrostatically adhere.

B. Liquid metal patterning

Galinstan (Geratherm, Germany) alloy consisting of approximately 68% gallium, 22% indium, and 10% tin, with smaller amounts of Bi and/or Sb, was used for the patterning of LM interconnects. LM patterning was realized with a customized setup consisting of a table top robot, MYT50 (Mycronic, Täby, Sweden); pressure applied to a syringe cartridge was controlled by a precision dispenser Ultimus V (Nordson EFD, Ohio, USA); and the process was monitored by a digital microscope (Dino-Lite Europe, The Netherlands). Patterning was performed using two needles of different inner diameter, a custom-made glass capillary needle of inner diameter 150 µm (Polymicro Technologies/Molex, Phoenix, USA), and an Optimum® flexible dispensing tip (Nordson EFD, Ohio, USA) of inner diameter 360 µm.

In order to identify parameters within which continuous and uniform traces are dispensed a preliminary study on the stable pressure-print height relation was performed for both needles. Deposition speed was set to 1 mm/s for patterning. Liquid metal traces were printed at a set printing height (i.e. proximity of printing needle from the substrate surface), while increasing the pressure in the cartridge up to the point where the oxide layer yielded, forming droplets on the substrate. The procedure was repeated increasing the printing height in increments of 10 µm until the LM trace lost contact with the substrate. The inspection was performed three times for each of the dispensing needles. For a detailed map of the parameters for reliable dispensing, refer to Fig. 1 and Fig. 2. Based on the preliminary study and identified parameters of reliable dispensing a print repeatability test of five examination lines was subsequently performed. Characterization of the influence of print height and applied pressure on the geometry of deposited traces was evaluated.

The repeatability test was done by printing 3 cm traces at specific printing conditions across the stable pressure-print height area. The width and height of the traces were measured at three different spots along each trace with vertical scan interferometry (3D Optical Profiler ZYGO, AMETEK, Berwyn, USA) using 10x magnification. The values of width and height of the traces were averaged and supplemented by a deviation.

C. Patch fabrication

The devices were fabricated in batches of six on A4-sized substrates of thermoplastic polyurethane film supplied on a paper liner Inspire®2150 (TC Transcontinental, Wrexham, United Kingdom). Using a spray gun, highly conductive paste (124-36, Creative Materials, Ayer, USA) was after thinning sprayed, transferring epidermal electrode patterns on top of the film. The original formulation of the paste contains 80 wt% Ag/AgCl particles with ratio of 66:34. The consistency of the highly viscous paste was modified by adding a designated thinner (102-03, Creative Materials, Ayer, USA) in 1:1 weight ratio. Molex 0.5 mm Pitch SlimStack Plug connectors (555600207) soldered to copper clad polyimide laminate (Holders Technology, London, UK) with contact pads for the LM, were cut to size and glued to the polyurethane substrate using a silicone adhesive (Elastosil A07, Wacker Chemie, Munich, Germany). Positioning of the components was performed using an automated pick-and-place robot MY300DX (Mycronic AB, Sweden). Patterning of LM interconnects between the connector and the electrodes was achieved as described above using the Optimum® flexible dispensing tip (Nordson EFD, Ohio, USA) of inner diameter 360 µm. Patterning was done with 1.3 kPa of pressure and 60 µm print height. The encapsulation of the LM interconnects was performed using the same setup as for patterning LM, but using the silicone adhesive (Elastosil A07, Wacker Chemie, Munich, Germany). The print height was set at 1 mm and velocity 10 mm/s. A smooth flow tapered dispensing tip G22 (ID of 0.41 mm) (Fisnar, Germantown, USA) was used as a printing needle. The applied pneumatic pressure was set to 120 kPa. The material used as a skin adhesive is a medical grade soft silicone gel adhesive, Silbione 4645 (ELKEM Silicones, Oslo, Norway), that was selectively dispensed in the form of fringes around the circumference of the patch to maintain high breathability. The print height was set at 0.3 mm and velocity 10 mm/s. Optimum® SmoothFlow™ tapered dispensing tip G25 with an inner diameter of 250 µm (Nordson EFD, Ohio, USA) was used as a printing needle. The applied pneumatic pressure was set to 250 kPa. In order to establish a stabile electrical interface between the epidermal electrode and the skin, sensing hydrogel pads (AG625, Axelgaard Manufacturing, Fallbrook, USA) were attached to the Ag/AgCl electrodes.

D. Integration of electronics

A prototype of a sensor device for data acquisition and streaming via Bluetooth (ST Microelectronics, Italy) was reconfigured in a new, soft casing with a counter connector Molex 0.5 mm Pitch SlimStack PCB Receptacle (541020204) to fit the patch. To power the sensor device, a rechargeable lithium coin cell battery LIR2032 was used and cased in the same fashion.

III. Results and discussion

A. Liquid metal patterning

The constructed map of parameters serves as a springboard for defining specific process window of continuous and uniform dispensing and for the subsequent characterization of the influence of these parameters on the geometry of deposited traces.

The regions of dispensing modes mapped in Fig. 1 and Fig. 2, respectively, can be characterized as follows: a region of discontinuous dispensing refers to too low proximity of the needle to the substrate – results in no dispensing or dispensing with poor quality affecting conductive electrical performance. A region of low feeding pressure implies imperfect dispensing caused by too low pressure applied in a cartridge supplying LM adequately during dispensing process. In contrast, too high pressure applied in the cartridge causes the deposited LM channel held by the oxide shell to be overfilled. Therefore, the oxide skin yields and the dispensing process results in the uncontrolled formation of blobs of LM. If the distance between the printing needle and the substrate is too high, there is a loss of contact between the LM at the orifice of a needle and the substrate surface. The LM cannot be further sheared on top of the surface and the mode leads to necking along the deposited lines or completely losing contact resulting in dispensing of disjointed traces.

The parameters at which it was possible to deposit continuous traces and which overlapped in the inspections were determined as the region of stable dispensing parameters. These regions are marked with the black frame.

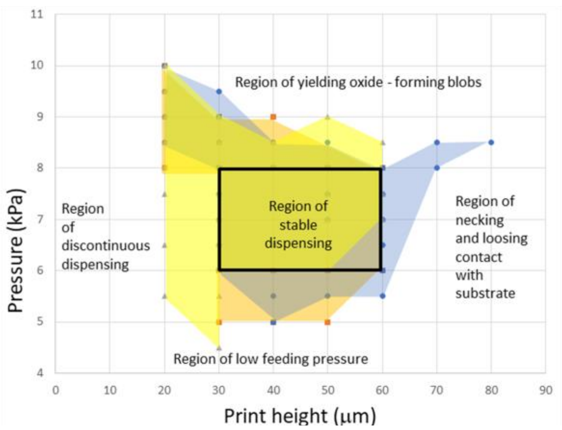

Fig. 1. Map of dispensing modes using 150 µm inner diameter printing needle with a region of stable dispensing marked with black frame.

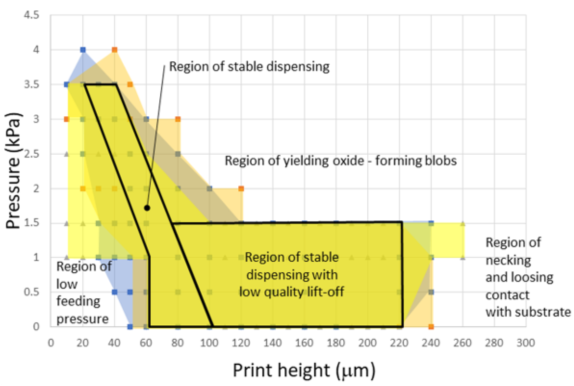

Fig. 2. Map of dispensing modes using 360 µm inner diameter printing needle with a region of stable dispensing marked with black frame.

In the case of the 150 µm ID needle, the stable printing region was defined to be between 30 and 60 µm of print height with 6 to 8 kPa of applied pressure. Furthermore, the influence of these parameters on the dimensions of printed lines deposited on a breathable polyurethane substrate was investigated, similar to previous studies by Cook et al. [14]. First of all, a constant print height of 45 µm with variable pressure of 6, 7 and 8 kPa. An analysis of dimensions of patterned traces as a function of pressure is plotted in Fig. 3 with an image of LM traces in Fig. 4. Further, a constant pressure of 7 kPa was determined with varying printing heights of 30, 40, 50 and 60 µm. Analysis of traces as a function of print height are plotted in Fig. 5 and depicted in Fig. 6.

The parameters of printing height and the applied pressure independently affect the geometry of the deposited structures. However, it is possible to observe a certain inconsistency in the geometry of the lines along their lengths, as evidenced by the standard deviation. This fact can be associated both with the deviation of the calibration of the exact print height, but also with LM wetting of the rugged surface topography of the polyurethane film. For surface analysis of used polyurethane film, see Fig. 7. However, the applied pressure significantly affects, both the dispensing itself and the finishing phase of printing. An appropriate combination of switching off the applied pressure with a sharp lift-off of the print head allows for the formation of smooth lines.

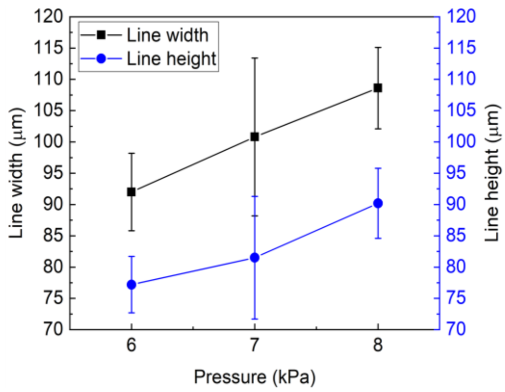

Fig. 3. Trace dimensions analysis of LM printed with 150 µm needle at constant print height of 45 µm and varying pressure.

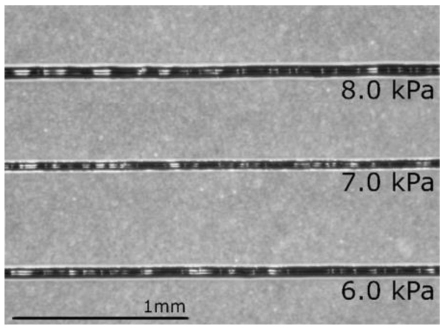

Fig. 4. Image of LM traces printed with 150 µm needle at constant print height of 45 µm and varying pressure.

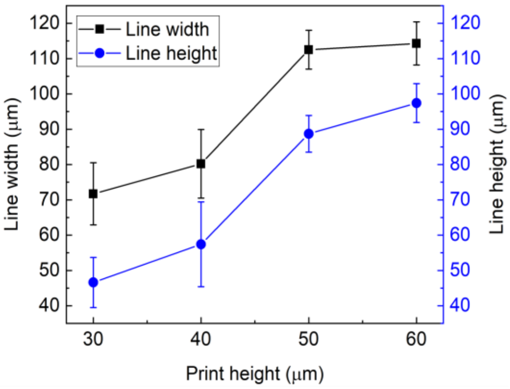

Fig. 5. Trace dimensions analysis of LM printed with 150 µm needle at constant pressure of 7 kPa and varying print heights

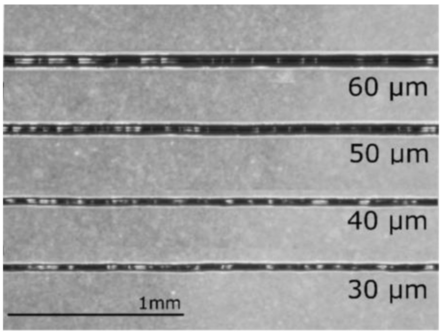

Fig. 6. Image of LM printed with 150 µm needle at constant pressure of 7 kPa and varying print heights

A similar analysis was performed using a printing needle with an inner diameter of 360 µm. Based on the mapped region of reliable dispensing, a constant print height of 60 µm was determined for the reproducibility test with varying applied pressure of 0.5, 1, 1.5 and 2 kPa. The analysis of the dimensions of the patterned traces as a function of pressure are plotted in Fig. 8 and Fig. 9. Analysis of traces as a function of print height are plotted and depicted in Fig. 10 and Fig. 11.

As previously reported [12, 14] and confirmed in our analysis, it is possible to reliably deposit and pattern LM traces using larger inner diameter printing needles at higher print heights, making the patterning technique less sensitive to eventual substrate unevenness. This is very important for large-scale deposition areas, A4 size as an example, for potential industrial adaptation. Our experience indicates a certain level of

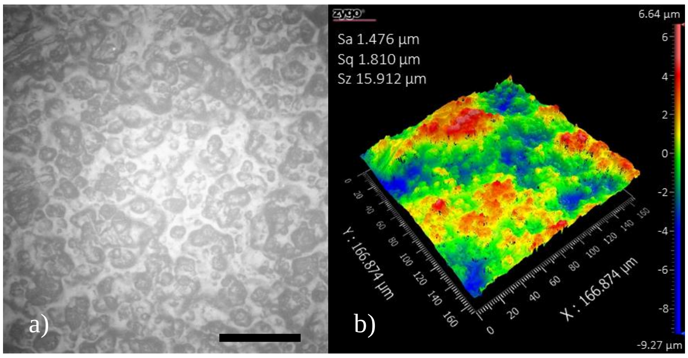

Fig. 7. Surface analysis of used polyurethane film (Inspire®2150, TC Transcontinental). a) Micrograph of surface and b) 3D topography of scanned surface. Scale bar corresponds to 50 µm.

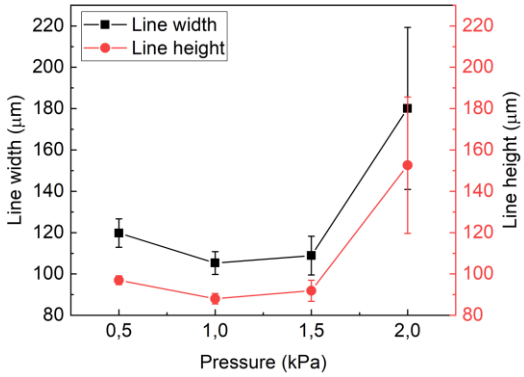

Fig. 8. Trace dimensions analysis of LM printed with 360 µm needle at constant print height of 60 µm and varying pressure.

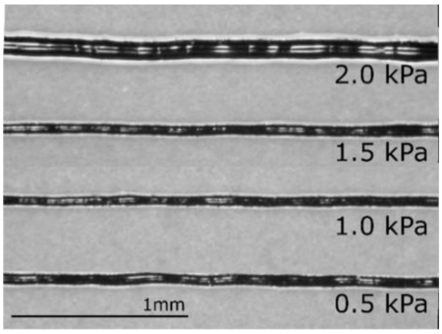

Fig. 9 Image of LM traces printed with 360 µm needle at constant print height of 60 µm and varying pressure

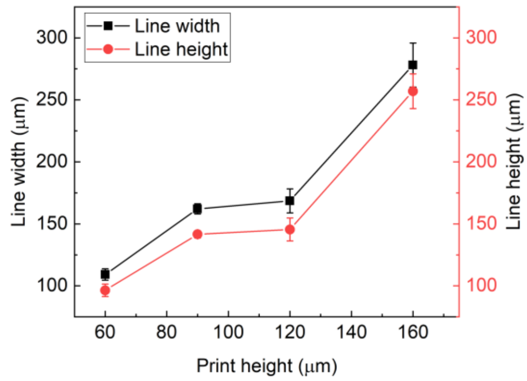

Fig. 10. Trace dimensions analysis of LM traces printed with 360 µm needle printed at constant pressure of 1 kPa and varying print heights

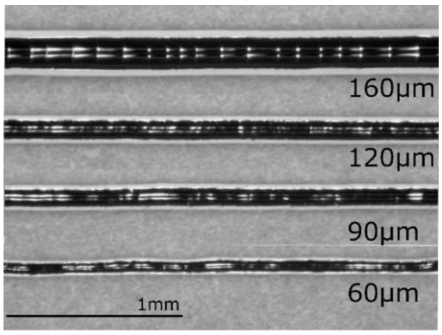

Fig. 11. Image of LM traces printed with 360 µm needle printed at constant pressure of 1 kPa and varying print heights.

sensitivity to pressure control of feeding pressure and places higher demands on the precision of pressure control. The waviness/corrugation along the deposited traces is observable especially on traces printed with the 360 µm needle and to some extent on traces printed with the 150 µm needle. According to our data, the waviness occurs when the printing height is less than one third of the inner diameter of the needle. This phenomenon may have a more complex cause, but indicates a more significant effect of surface roughness at lower printing heights. When printing with the 150 µm inner diameter needle, the geometry of the traces are highly dependent on print height. A lower print height results in traces with high width/height ratio significantly, see Fig. 12. It should also be noted that the deviation from the mean width/height ratio is larger for the traces printed at lower heights due to the relative change of height related to unevenness of the surface. This deviation relates to the shearing mechanism of LM on top on surface with increased surface roughness. The surface of increased roughness results in inconsistent wetting by LM, and thereby an uneven trace width [16 - 17]. We assume that for ultra-high-resolution dispensing using needles with lower inner diameters, surface topography and associated roughness can have significant impact. Depositing LM at higher print heights, both with the 150 µm needle and the 360 µm needles, results in lower width/height ratio and smaller deviations from the mean, Fig. 12 and Fig. 13, respectively. This indicates a mechanism in which the interface between the substrate surface and the sheared LM is smaller and therefore LM forms a stable tubular filament-like geometry.

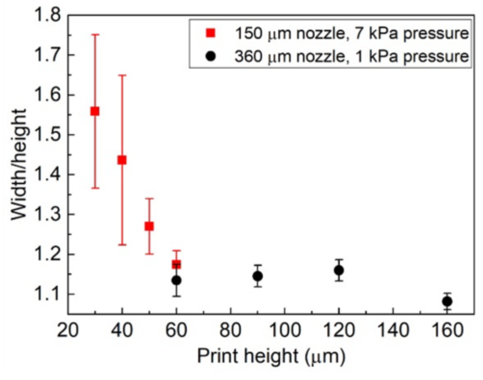

Fig. 12. Width/height aspect ratio relation for the printed traces at constant pressure

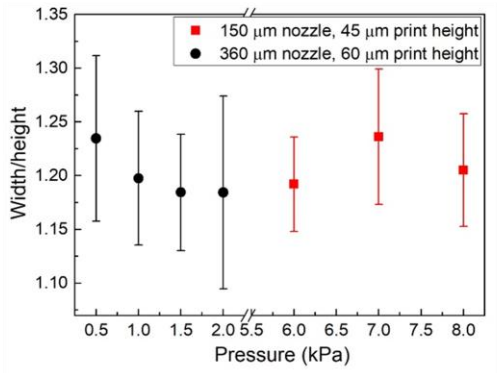

Fig. 13. Width/height aspect ratio relation for the printed traces at constant print height.

B. *Wearable patch functioning*

The functionality of the fabricated wearable sensor device consisting of the wearable patch with LM interconnects and modular electronics depicted in the Fig. 14 was tested by connecting the modules with the patch and first applied on the forearm skin of a male wearer, Fig. 15. Wearing aspects, such as adhesion to the skin, suitable pressing of the electronic modules to the skin, and overall unobtrusiveness under the clothing over a longer wearing period, were taken into consideration. Furthermore, the aspect of wireless connection, data acquisition and transmission were verified.

For real-time electrocardiography (ECG) monitoring, the wearable sensor device was applied in the middle of the top of the abdomen of a male wearer as illustrated in Fig. 16 with a section of the electrocardiogram collected from the wearable patch.

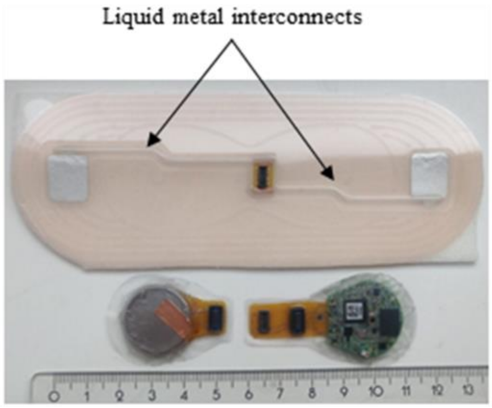

Fig. 14. A photograph of the wireless wearable device consisting of electronic modules and soft and stretchable sensor patch with patterned liquid metal interconnects.

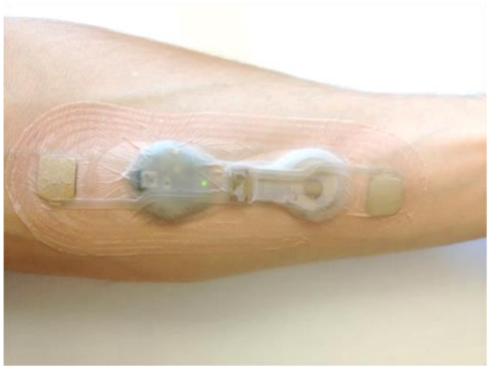

Fig. 15. A photograph of attached wireless sensor patch on forearm skin for demonstration.

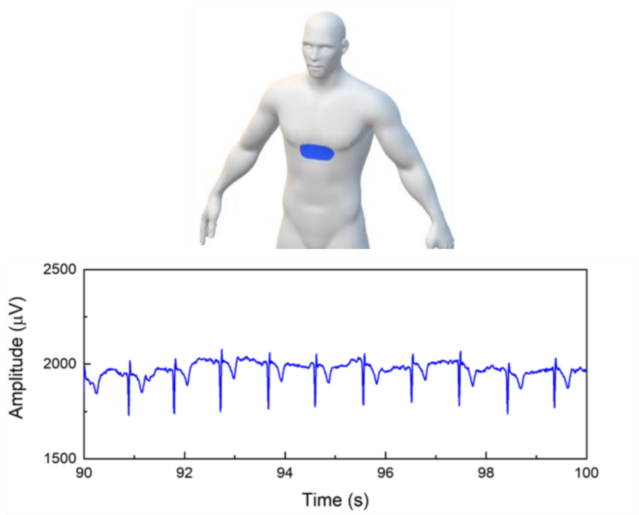

Fig. 16. Positioning of the wearable sensor patch in the middle of the top of the abdomen marked as a blue area with an example of monitored electrocardiogram.

IV. Conclusion

We inspected and demonstrated LM patterning technique on a non-silicone elastomeric substrate with considerable breathability. The investigation of dispensing parameters for 150 µm and 360 µm inner diameter needles provides a reference to reliably pattern LM on a porous and rough surface. However, the precision and repeatability of patterning are subject to previously reported conditions such as surface uniformity, evenness and cleanliness. To overcome surface unevenness across larger deposition areas, dispensing needles of higher inner diameters offer a simple solution for potential scaled-up manufacturing. The digitally patterned LM traces were incorporated as compliant electrical interconnects in the design of the wearable device. The fabricated soft, stretchable and breathable sensor patch exhibited the ability to monitor electrocardiography and wirelessly stream the signal in real-time which proved the high potential for applications in sport and healthcare.

Acknowledgment

The authors would like to thank Klara Björnander Rahimi for her contribution in the initial stage of the work, Elvis Carlsson for guidance and assistance with pick and place technology, and TC Transcontinental UK for providing sample materials.

This research was funded by the European Union's Horizon 2020 research and innovation programme under grant agreement No 824984 - Soft intelligence epidermal communication platform (SINTEC).

References

[1] S. Xu, A. Jayaraman, and J.A. Rogers, "Skin sensors are the future of health care," Nature, vol. 571(7765), pp. 319-321, July 2019.

[2] K.Y. Kwon, Y.J. Shin, J.H. Shin, et al., "Stretchable, Patch-Type Calorie-Expenditure Measurement Device Based on Pop-Up Shaped Nanoscale Crack-Based Sensor," Adv. Healthc. Mater., vol. 8(19), October 2019.

[3] H.U. Chung, B.H. Kim, J.Y. Lee, et al., "Binodal, wireless epidermal electronic systems with in-sensor analytics for neonatal intensive care," Science, vol. 363(6430) eaau0780, March 2019.

[4] J. Alberto, C. Leal, C. Fernandes, et al., "Fully Untethered Battery-free Biomonitoring Electronic Tattoo with Wireless Energy Harvesting," Sci. Rep., vol. 10, pp. 5539, March 2020.

[5] K.D. Harris, A.L. Elias, and H.-J. Chung, "Flexible electronics under strain: a review of mechanical characterization and durability enhancement strategies," J. Mater. Sci., vol. 51, pp. 2771–2805, March 2016.

[6] K.-I. Jang, K. Li, H. Chung, et al., "Self-assembled threedimensional network designs for soft electronics," Nat. Commun. vol. 8, pp. 15894, June 2017.

[7] S. Jeong, K. Hjort, and Z. Wu, "Tape Transfer Atomization Patterning of Liquid Alloys for Microfluidic Stretchable Wireless Power Transfer," Sci. Rep., vol. 5, pp. 8419, February 2015.

[8] B. Wang, J. Gao, J. Jiang, Z. Hu, K. Hjort, Z. Guo, and Z. G. Wu, "Liquid Metal Microscale Deposition enabled High Resolution and Density Epidermal Microheater for Localized Ectopic Expression in Drosophila," Adv. Mater. Technol., vol. 7, pp. 2100903, March 2022.

[9] G. Li, X. Wu and D.-W. Lee, "A galinstan-based inkjet printing system for highly stretchable electronics with self-healing capability," Lab on a chip, vol. 16(8), pp. 1366-1373, March 2016.

[10] J.W. Boley, E.L. White, G.T.-C Chiu, and R.K. Kramer, "Direct Writing of Gallium-Indium Alloy for Stretchable Electronics," Adv. Funct. Mater., vol. 24, pp. 3501-3507, February 2014.

[11] Y. Yoon, S. Kim, D. Kim, S.K. Kauh, J. Lee, "Four Degrees-of-Freedom Direct Writing of Liquid Metal Patterns on Uneven Surfaces," Adv. Mater. Technol., vol. 4(2), pp. 1800379, October 2018.

[12] S. Kim, J. Oh, D. Jeong, W. Park, and J. Bae, "Consistent and Reproducible Direct Ink Writing of Eutectic Gallium–Indium for High-Quality Soft Sensors," Soft Robotics, vol. 5(5), pp. 601-612, October 2018.

[13] K. Doudrick, S. Liu, E. M. Mutunga, K. L. Klein, V. Damle, K. K. Varanasi, and Konrad Rykaczewski, "Different Shades of Oxide: From Nanoscale Wetting Mechanisms to Contact Printing of Gallium-Based Liquid Metals," Langmuir, vol. 30(23), pp. 6867-6877, May 2014.

[14] A. Cook, D.P. Parekh, C. Ladd, G. Kotwal, L. Panich, M. Durstock, M.D. Dickey and C.E. Tabor, "Shear-Driven Direct-Write Printing of Room-Temperature Gallium-Based Liquid Metal Alloys," Adv. Eng. Mater., vol. 21(11), pp. 1900400, July 2019.

[15] M.D. Dickey, R.C. Chiechi, R.J. Larsen, E.A. Weiss, D.A. Weitz, and G.M. Whitesides, "Eutectic Gallium-Indium (EGaIn): A Liquid Metal Alloy for the Formation of Stable Structures in Microchannels at Room Temperature," Adv. Funct. Mater., vol. 18, pp. 1097-1104, 2008.

[16] R.K. Kramer, J.W. Boley, H.A. Stone, J.C. Weaver, and R.J. Wood, "Effect of microtextured surface topography on the wetting behavior of eutectic gallium-indium alloys," Langmuir, vol. 30 (2), pp. 533-539, January 2014.

[17] I.D. Joshipura, H. R. Ayers, G. A. Castillo, C. Ladd, C. E. Tabor, J. J. Adams, and M. D. Dickey, "Patterning and Reversible Actuation of Liquid Gallium Alloys by Preventing Adhesion on Rough Surfaces," ACS Applied Materials & Interfaces, vol. 10 (51), pp. 44686-44695, 2018.